

Supporting information

Heterogeneous H₂O₂-based selective oxidations over zirconium tungstate α -ZrW₂O₈

Vasilii Yu. Evtushok,¹ Irina D. Ivanchikova,¹ Olga V. Zalomaeva,¹ Alexander I. Gubanov,²
Boris A. Kolesov,² Tatiana S. Glazneva,¹ Oxana A. Kholdeeva^{1,*}

¹Boreskov Institute of Catalysis, Pr. Lavrentieva 5, Novosibirsk 630090, Russia

²Nikolaev Institute of Inorganic Chemistry, Pr. Lavrentieva 3, Novosibirsk 630090, Russia

* Corresponding author: khold@catalysis.ru

Table of Contents

Catalyst characterisation	p. 2
Table S1. EDX data for ZrW ₂ O ₈ -A	p. 2
Figure S1. PXRD patterns of ZrW ₂ O ₈ -A and ZrW ₂ O ₈ -D	p. 2
Figure S2. PXRD patterns of ZrW ₂ O ₈ -A and ZrW ₂ O ₈ -A after H ₂ O ₂ treatment under conditions similar to epoxidation reactions	p. 2
Figure S3. Adsorption isotherms of ZrW ₂ O ₈ -A before and after cyclooctene oxidation reaction	p. 3
Table S2. N ₂ adsorption data for ZrW ₂ O ₈ -A before and after cyclooctene oxidation reaction	p. 3
Figure S4. SEM images of ZrW ₂ O ₈ -D	p. 4
Figure S5. IR spectra of ZrW ₂ O ₈ -A immediately after calcination at 500 °C and after prolonged exposure to air	p. 5
Figure S6. Raman spectra of ZrW ₂ O ₈ -A, -B, -C, and -D immediately after calcination at 500 °C	p. 5
Figure S7. Raman spectra of ZrW ₂ O ₈ -A, ZrW ₂ O ₈ -B, and ZrW ₂ O ₈ -D before and after addition of 15 wt. % aqueous H ₂ O ₂	p. 6
Catalytic properties of ZrW₂O₈	p. 7
Figure S8. Kinetic curves for a) H ₂ O ₂ decomposition over ZrW ₂ O ₈ -A in the absence of organic substrate at 30-70 °C and b) CyO epoxidation over ZrW ₂ O ₈ -A	p. 7
Figure S9. Hot catalyst filtration test for oxidative cleavage of <i>trans</i> -cyclohexanediol	p. 7
Table S3. Effect of water, acid and base additives on CyO epoxidation with H ₂ O ₂ over ZrW ₂ O ₈	p. 8
Table S4. Structures of alkenes and corresponding products for Tables 6 and 7	p. 9
Table S5. Effect of solvent on 3-carene oxidation with H ₂ O ₂ over ZrW ₂ O ₈	p. 10

Catalyst characterisation

Table S1. EDX data for $\text{ZrW}_2\text{O}_8\text{-A}$.

Element	Weight %	Atomic %
O K	22.78	73.17
Zr L	18.47	10.41
W M	58.75	16.43

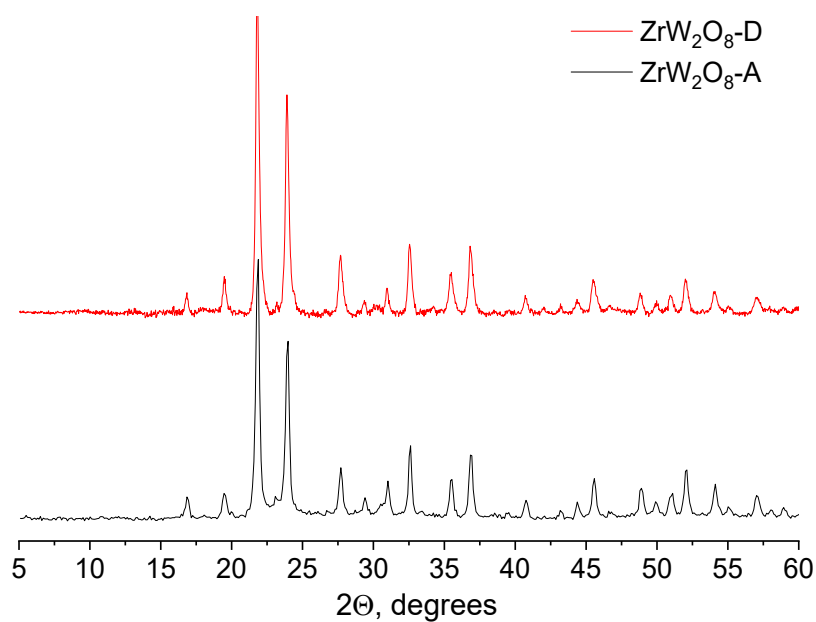


Figure S1. PXRD patterns of $\text{ZrW}_2\text{O}_8\text{-A}$ and $\text{ZrW}_2\text{O}_8\text{-D}$.

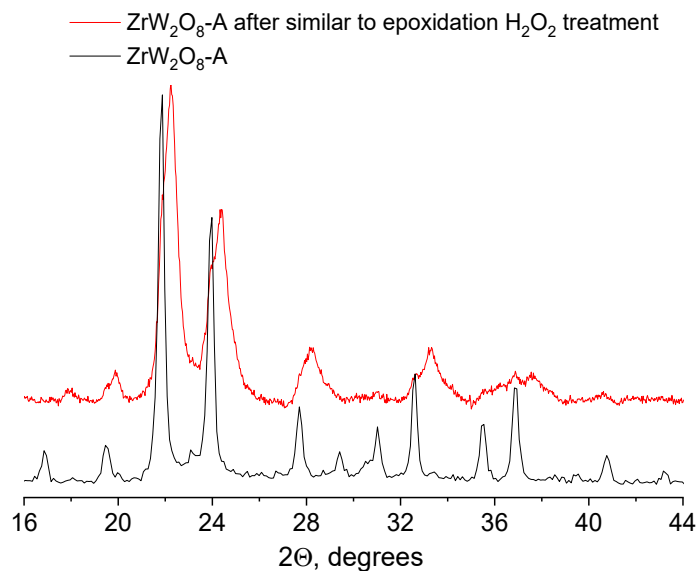


Figure S2. PXRD patterns of $\text{ZrW}_2\text{O}_8\text{-A}$ and $\text{ZrW}_2\text{O}_8\text{-A}$ after H_2O_2 treatment under conditions similar to epoxidation reactions ($\text{ZrW}_2\text{O}_8\text{-A}$ 0.300 g, $[\text{H}_2\text{O}_2] = 0.2$ M, CH_3CN 10 mL, 120 min, 50°C).

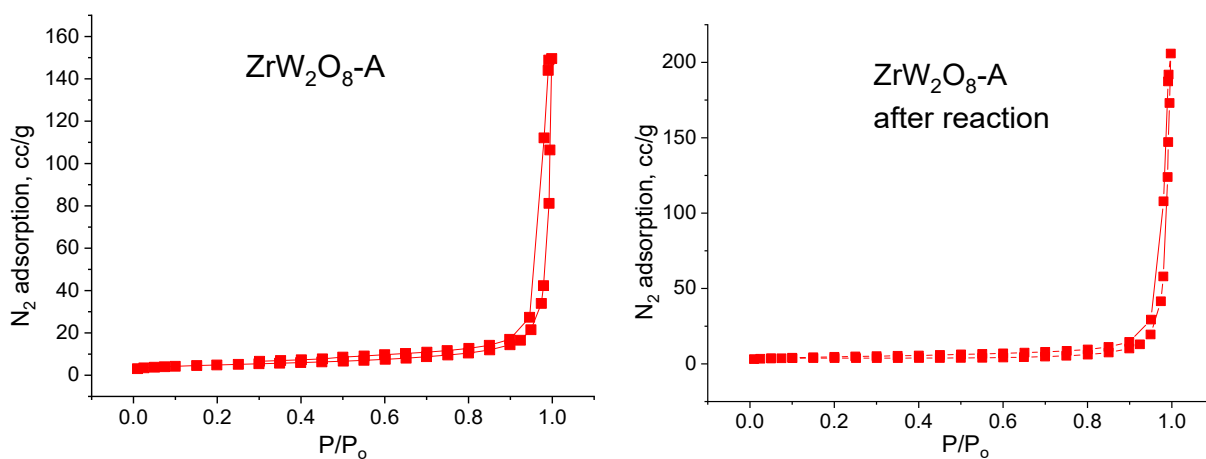


Figure S3. Adsorption isotherms of $\text{ZrW}_2\text{O}_8\text{-A}$ before and after cyclooctene oxidation reaction (Reaction conditions: $[\text{CyO}] = 0.1 \text{ M}$, $[\text{H}_2\text{O}_2] = 0.2 \text{ M}$, $\text{ZrW}_2\text{O}_8\text{-A}$ 30 mg, CH_3CN 1 mL, $50 \text{ }^\circ\text{C}$).

Table S2. N_2 adsorption data for $\text{ZrW}_2\text{O}_8\text{-A}$ before and after cyclooctene oxidation reaction.

	$\text{ZrW}_2\text{O}_8\text{-A}$	$\text{ZrW}_2\text{O}_8\text{-A}$ after reaction
S_{BET} , m^2/g	17	15
V_{micro} , cc/g	0.001(t-plot)/0.001(DFT)	0.004(t-plot)/0(DFT)
V_{meso} , cc/g	0.051(DFT)/0.037(BJH)	0.062(DFT)/0.045(BJH)

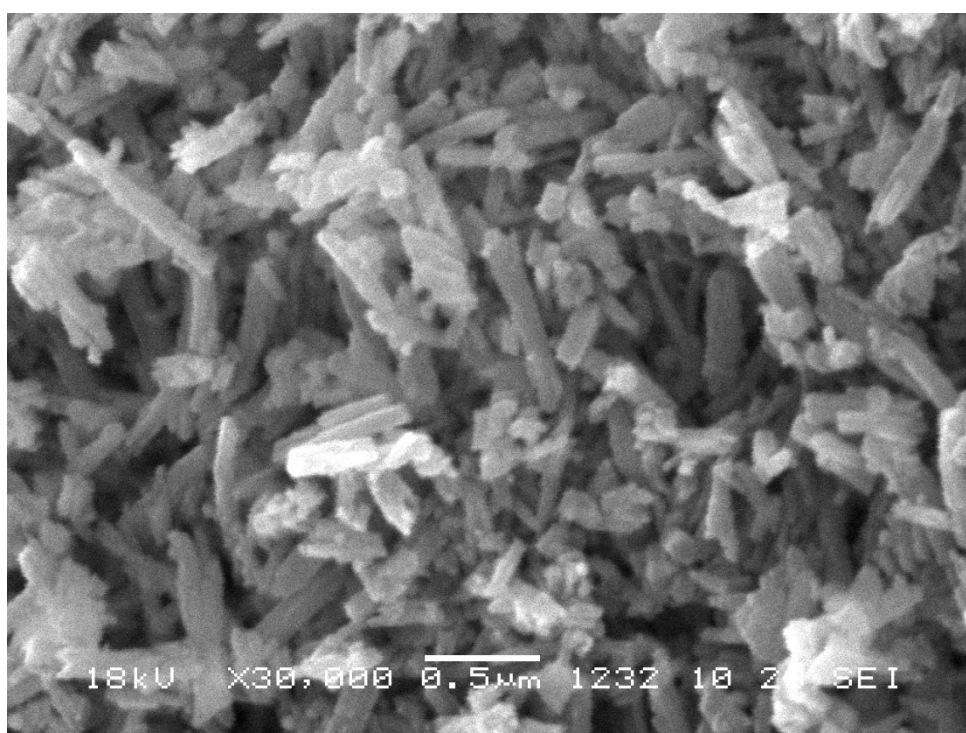
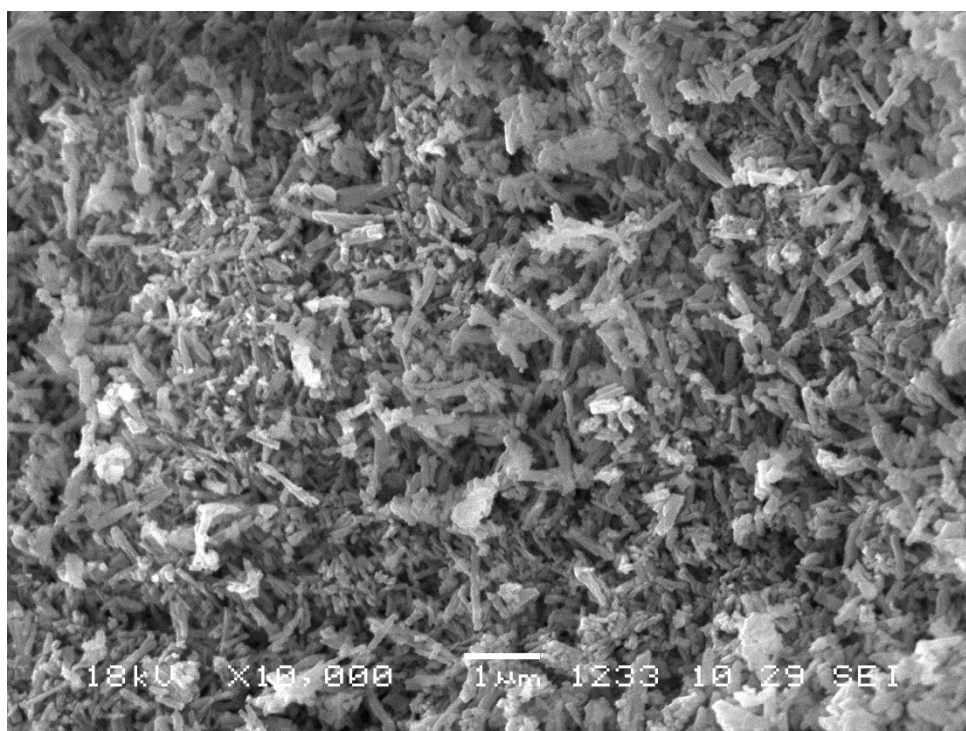


Figure S4. SEM images of ZrW₂O₈-D.

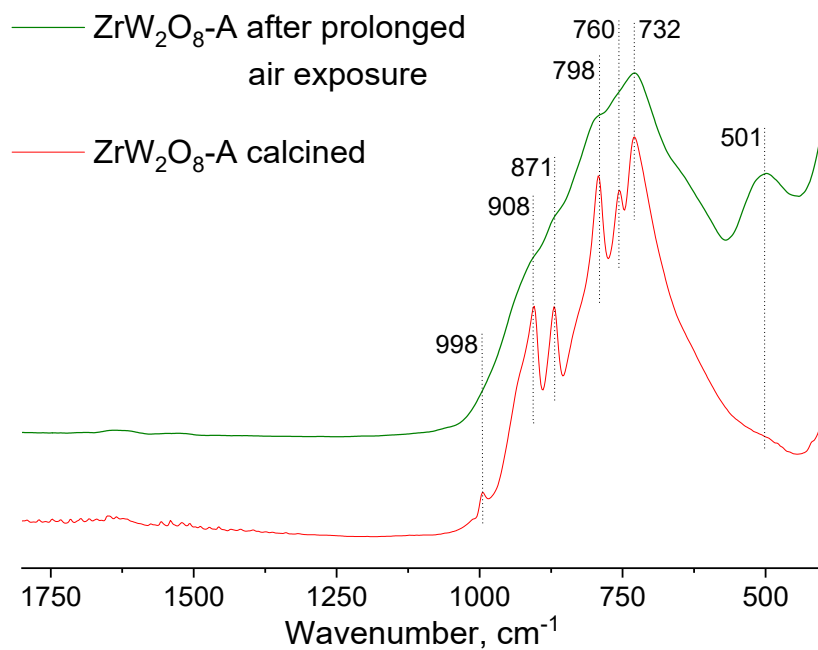


Figure S5. IR spectra of ZrW₂O₈-A immediately after calcination at 500 °C and after prolonged exposure to air.

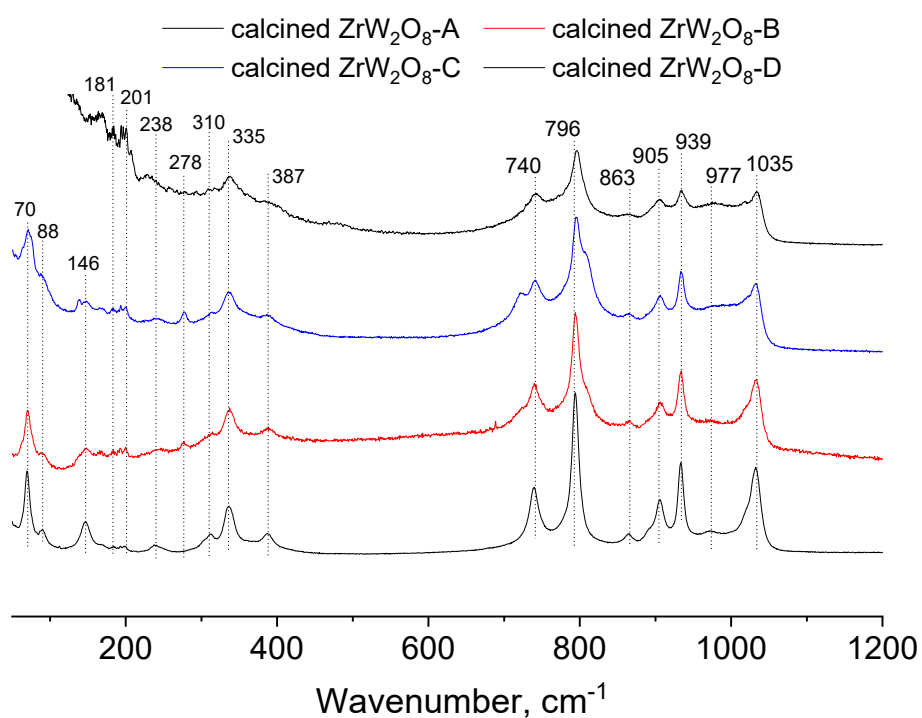


Figure S6. Raman spectra of ZrW₂O₈-A, -B, -C, and -D immediately after calcination at 500 °C.

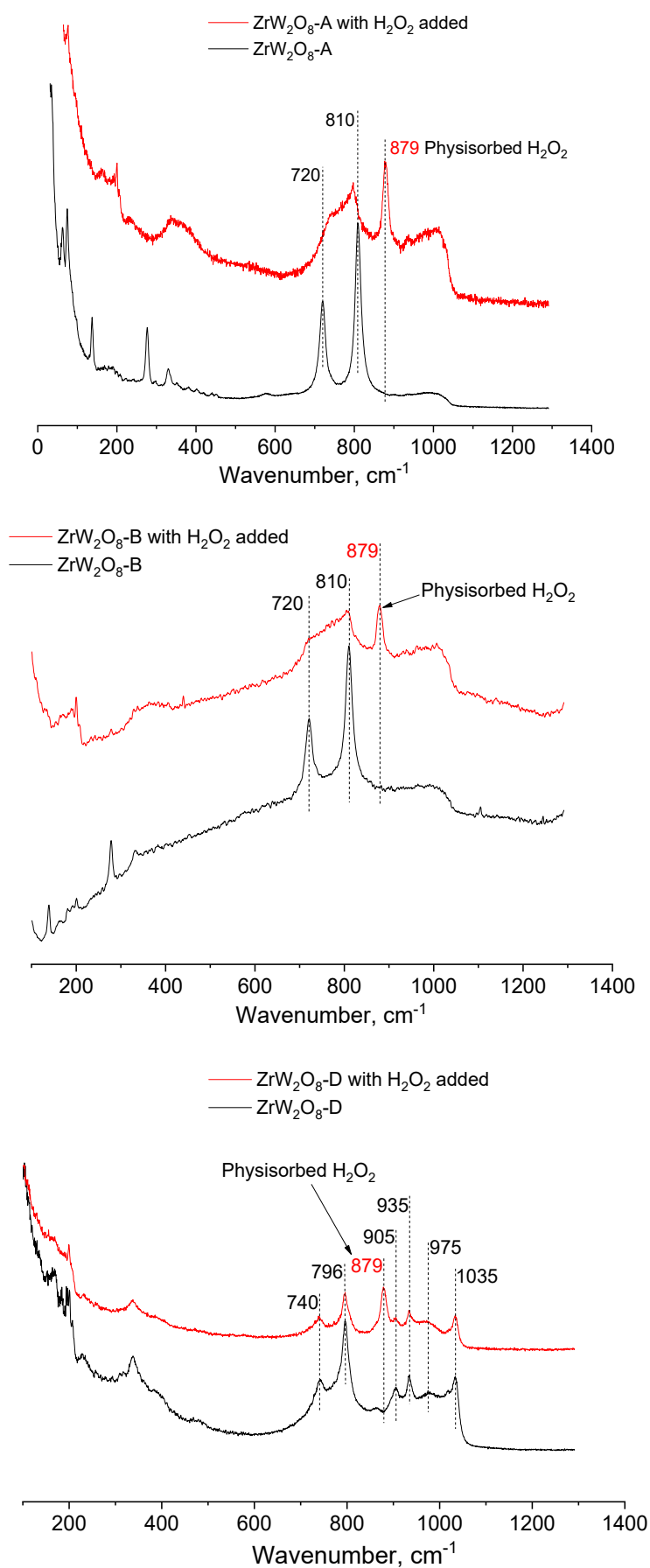


Figure S7. Raman spectra of ZrW₂O₈-A, ZrW₂O₈-B, and ZrW₂O₈-D before and after addition of 15 wt. % aqueous H₂O₂.

Catalytic properties of ZrW_2O_8

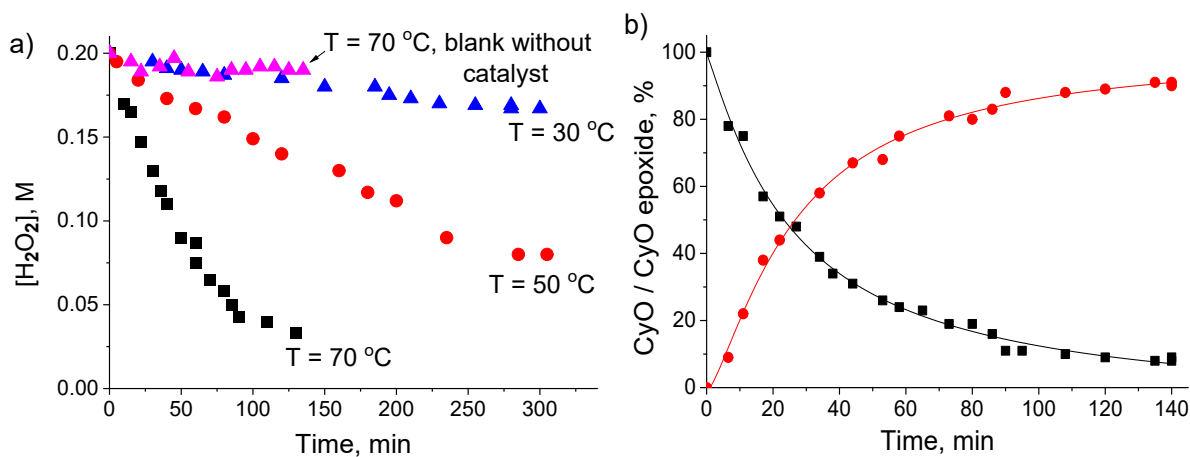


Figure S8. Kinetic curves for a) H_2O_2 decomposition over ZrW_2O_8 -A in the absence of organic substrate at 30-70 °C (Reaction conditions: $[\text{H}_2\text{O}_2] = 0.2$ M, ZrW_2O_8 -A 0.180 g, CH_3CN 6 mL) and b) CyO epoxidation over ZrW_2O_8 -A (Reaction conditions: $[\text{CyO}] = 0.1$ M, $[\text{H}_2\text{O}_2] = 0.2$ M, ZrW_2O_8 -A 0.030 g, CH_3CN 1 mL, 50°C).

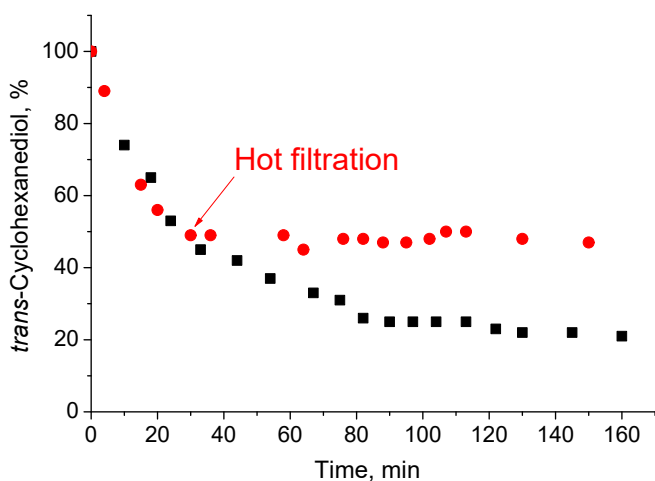


Figure S9. Hot catalyst filtration test for oxidative cleavage of *trans*-cyclohexanediol. Reaction conditions: $[\text{CH-diol}] = 0.1$ M, $[\text{H}_2\text{O}_2] = 0.8$ M, ZrW_2O_8 -B 0.030 g, CH_3CN 1 mL, 70°C .

Table S3. Effect of water, acid and base additives on CyO epoxidation with H₂O₂ over ZrW₂O₈

Entry	Additive, mmol	Conversion CyO, %	Select. Epoxide ^a , %
1 ^b	none	86	98
2	none	90	98
3	H ₂ O 0.1	90	98
4	H ₂ O 0.5	87	85
5	H ₂ O 1.0	85	80
6	HClO ₄ 0.05	88	5 ^c
7	HClO ₄ 0.005	87	63
8 ^d	HClO ₄ 0.005	57	5
9	NaOAc 0.05	50	1-2 ^c
10	NaOAc 0.005	33	48
11 ^d	NaOAc 0.005	30	5

Reaction conditions: [CyO] = 0.1 M, [H₂O₂] = 0.2 M, [H₂O] = 0.7–1.7 M, catalyst ZrW₂O₈-A 0.030 g, CH₃CN 1 mL, 120 min, 50 °C.

^a Epoxide yield based on substrate consumed.

^b 77 wt.% H₂O₂ was employed instead of 30% H₂O₂, [H₂O] = 0.125 M.

^c Numerous unidentified side-products.

^d Blank experiments without ZrW₂O₈ catalyst.

The calculation of the relevant amount of additives was made on the assumption that there is one active site per 9.2×9.2 Å unit cell area. Taking into account the surface area of the sample determined from low-temperature N₂ adsorption data (Table S2), we could then estimate that the content of active sites in ZrW₂O₈ is about 30 μmol/g. The addition of small amounts of HClO₄ (0.005 mmol, which is roughly 5 equiv. relative to the estimated number of active sites on the surface of 30 mg of ZrW₂O₈) reduced the epoxide selectivity quite strongly while, with large amounts of acid (0.05 mmol), selectivity was almost zero and a large number of unidentified products was formed. At the same time, the achievable conversion and reaction rate remained practically unchanged, which suggests that the acid apparently does not protonate the active centres. As in the case of increasing water concentration, the reason for the decrease in selectivity is, most likely, acceleration of side reactions involving the epoxide.

On the other hand, small additives of basic sodium acetate led to strong decrease in the conversion, reaction rate, and selectivity (Table S4). The inhibitory effect of sodium acetate could be related to possible deprotonation of active sites, but this seems unlikely, since separate treatment of the catalyst with sodium acetate did not lead to any change in its catalytic characteristics. We may assume that the inhibitory effect of base is probably related to the strong adsorption of acetate on the active sites.

Table S4. Structures of alkenes and corresponding products for Tables 6 and 7.

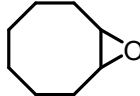
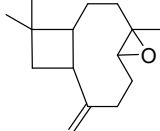
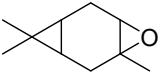

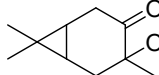
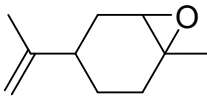
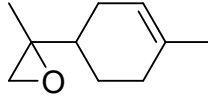
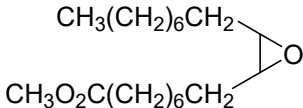
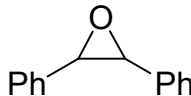

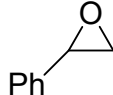
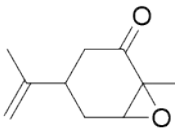
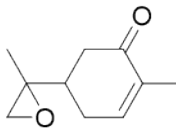
Substrate	Main products
Cyclooctene	
Caryophyllene	
3-Carene	   e -diol -olon epoxid
Limonene	  1,2-epoxide (endo) 7,8-epoxide (exo)
Methyl oleate	
<i>cis</i> -Stilbene	 cis-epoxide
<i>trans</i> -Stilbene	 trans-epoxide
Styrene	
Carvone	  1,2-epoxide (endo) 7,8-epoxide (exo)

Table S5. Effect of solvent on 3-carene oxidation with H₂O₂ over ZrW₂O₈

Solvent	Time, min	3-Carene Conversion, %	Epoxide Yield / Selectivity, ^a %	-diol + -olon Yield / Selectivity, ^a %
MeCN	240	30	17 / 57	4 / 13
DMC	180	37	4 / 11	22 / 59
EtOAc	180	31	4 / 13	20 / 65

Reaction conditions: [3-carene] = 0.1 M, [H₂O₂] = 0.2 M, ZrW₂O₈-A 0.015 g, solvent 1 mL, 50 °C.

^a Yield based on 3-carene converted.